Influence of the anisotropy of the positron wave function on the calculation of the momentum density of positron annihilation pairs

H. Sormann
Institut für Kernphysik, Technische Universität Graz, Petersgasse 16, A-8010 Graz, Austria
(Received 16 July 1990; revised manuscript received 20 November 1990)

Using the augmented-plane-wave band-structure method, the reliability of approximation formulas for the momentum density of positron annihilation pairs (MDAP) is investigated for some alkali metals and for Cu and Pd. Such formulas are often based on neglecting the anisotropy of the positron wave function. A comparison of two of these approximations (proposed by Loucks and Hubbard-Mijnarends) with an improved one that is presented here indicates that the complete or partial neglect of the anisotropy of ψ_+ has almost no influence on the MDAP for momenta within the central Brillouin zone and only weak influence within the nearest umklapp zones. For higher momenta, however, large errors may appear, especially if one investigates annihilation processes with highly delocalized valence electrons.

I. INTRODUCTION

During recent years, many theoretical investigations have dealt with the important role of the positron wave function ψ_+ for an accurate and reliable determination of the momentum density of positron annihilation pairs (MDAP) in crystalline solids. Practically all well-proved solid-state approaches have been applied to the problem of getting positron wave functions with the following properties. They should (1) lead to MDAP formulas which are not too complicated for practical purposes and (2) describe the physics of the positron (especially the anisotropy of ψ_+) within the whole volume of the crystal as exactly as possible .

In fact, it is rather difficult to calculate positron wave functions which simultaneously fulfill these two conditions. For example, both the Wigner-Seitz approximation[1] and the plane-wave (PW) expansion[2-4] of ψ_+ lead to relatively simple expressions for the MDAP, but the former approximation does not at all take into account the anisotropy of the wave function, while the latter shows a very poor convergence for small values of r.

A successful compromise between the two conditions mentioned above is offered by the pseudopotential method[5-7] where the positron wave function is described by a product of a rapidly varying core function and a smooth pseudowave function (which can be effectively expanded into plane waves), and the augmented-plane-wave[8-14] (APW) method. The application of the linearized form of the Korringa-Kohn-Rostocker-Ziman (KKRZ) method—developed by Hubbard[15] and by Hubbard and Mijnarends[16]—to MDAP calculations also leads to APW-type expressions.[17,18] How and to what extent the APW-type MDAP formulas take into account the anisotropy of ψ_+ will be discussed in detail in Sec. III. The problem is that realistic representations of the positron wave function frequently lead to very complicated MDAP formulas. Therefore, in many APW-type approaches, ψ_+ is assumed to be spherically symmetrical, at least within the muffin-tin sphere. A similar and very successful concept for MDAP calculations uses the linear-muffin-tin orbitals (LMTO) approach:[19] Inside a sphere with Wigner-Seitz radius (overlapping spheres), ψ_+ is approximated by its spherical average, and a plane-wave expansion for the product of the electron and the positron wave function is used in the overlap correction terms.

Another way of calculating the momentum density in Compton scattering and positron annihilation is based on the Koringa-Kohn-Rostocker (KKR) method and a multiple-scattering formalism.[20,21] The corresponding formula which takes into account the full anisotropy of ψ_+ is relatively complicated but nevertheless well suited for computational evaluations.[20,22] Finally, linear combinations of atomiclike orbitals (LCAO) methods have also been successfully applied to this problem,[23] leading to MDAP formulas which also include anisotropic positron wave functions, due to the fact that ψ_+ is represented by a sum of orbital functions centered at different atomic sites. However, the numerical expense of these methods is rather high. For more details, see, e.g., the review articles Refs. 18 and 24 and the references therein.

Recently, we published a paper[25] where we investigated the sensitivity of the MDAP within the independent-particle model (IPM) to the electron and positron crystal potentials using the APW method. We were especially interested in the high-momentum components of the MDAP, and we observed that for a proper description of some of these components, the spatial anisotropy of the positron wave function must not be neglected.

Motivated by this experience, we started the following investigation on the reliability of APW-based MDAP formulas which are often used in the literature. De-

spite the fact that the work presented here uses a specific band-structure approach, some of its results (concerning the influence of the anisotropy of ψ_+ on the calculated higher-momentum umklapp components of the MDAP) may also be of some interest for users of other methods to calculate electron and positron wave functions.

II. BASIC RELATIONS

In the framework of the IPM, the MDAP is given by[17]

$$\rho_{\mathrm{IPM}}(\mathbf{p}) = 2\sum_{n,\mathbf{k}} f(n,\mathbf{k})|A_n(\mathbf{k},\mathbf{p})|^2 , \tag{1}$$

with

$$A_n(\mathbf{k},\mathbf{p}) = \frac{V}{\Omega}\delta(\mathbf{p}-\mathbf{k}-\mathbf{K})\int_\Omega d\mathbf{r}\exp(-i\mathbf{p}\cdot\mathbf{r})\psi_{n\mathbf{k}}(\mathbf{r})\psi_+(\mathbf{r}) , \tag{2}$$

where $\hbar\mathbf{p}$ represents the photon-pair momentum, $f(n,\mathbf{k})$ denotes the Fermi-Dirac distribution function, and the factor 2 accounts for the spin degeneracy. $\psi_{n\mathbf{k}}$ and ψ_+ are the wave functions of the annihilated electron and of the thermalized positron, respectively, both normalized to the crystal volume V. Ω is the volume of the primitive cell, and $\mathbf{K}$ denotes a reciprocal-lattice vector such that $\mathbf{p}-\mathbf{K}$ lies in the first Brillouin zone (BZ). In the following, all electron and positron wave functions are given as APW expansions. For the crystal potentials seen by the electrons, self-consistent muffin-tin potentials including the local Hedin-Lundqvist correlation term[26] were used. In the case of the alkali metals and copper, these potentials were obtained from our own APW calculations, and for palladium, the potential published by Moruzzi, Janak, and Williams[27] was used. The crystal potentials for the positrons were simply the Coulomb parts of the corresponding electron potentials (without the exchange-correlation terms) with opposite sign. No electron-positron correlation was included.

For crystal lattices without a basis (and only such materials are investigated in this paper), the electron wave functions are given by

$$\psi_{n\mathbf{k}}(\mathbf{r}) = \frac{1}{\sqrt{V}}\sum_{\mathbf{G}} a_{\mathbf{G}}(\mathbf{k})\,\exp[i(\mathbf{k}+\mathbf{G})\cdot\mathbf{r}] \quad \text{for } |\mathbf{r}| > r_{\mathrm{MT}} , \tag{3}$$

$$\psi_{n\mathbf{k}}(\mathbf{r}) = \frac{1}{\sqrt{V}}\sum_{\mathbf{G}} a_{\mathbf{G}}(\mathbf{k})\,4\pi\sum_{\ell,m}^{\ell_{\max}} i^\ell j_\ell(|\mathbf{k}+\mathbf{G}|r_{\mathrm{MT}}) \times\frac{R_\ell(r,E_n)}{R_\ell(r_{\mathrm{MT}},E_n)} \times Y^*_{\ell m}(\mathbf{k}+\mathbf{G})Y_{\ell m}(\mathbf{r}) \quad \text{for } |\mathbf{r}| \le r_{\mathrm{MT}} . \tag{4}$$

Correspondingly, the formulas for the positron wave function in its quantum-mechanical ground state read

$$\psi_+(\mathbf{r}) = \frac{1}{\sqrt{V}}\sum_{\mathbf{G}} b_{\mathbf{G}}\,\exp(i\mathbf{G}\cdot\mathbf{r}) \quad \text{for } |\mathbf{r}| > r_{\mathrm{MT}} , \tag{5}$$

$$\psi_+(\mathbf{r}) = \frac{1}{\sqrt{V}}\sum_{\mathbf{G}} b_{\mathbf{G}}\,4\pi\sum_{\ell,m}^{\ell_{\max}} i^\ell j_\ell(|\mathbf{G}|r_{\mathrm{MT}}) \times\frac{R_{+,\ell}(r,E_+)}{R_{+,\ell}(r_{\mathrm{MT}},E_+)} \times Y^*_{\ell m}(\mathbf{G})Y_{\ell m}(\mathbf{r}) \quad \text{for } |\mathbf{r}| \le r_{\mathrm{MT}} . \tag{6}$$

In order to distinguish this positron wave function from the approximations which are discussed in the following, throughout this paper, Eqs. (5) and (6) are called the "true" APW positron wave function.

In Eqs. (3) – (6), the $a_{\mathbf{G}}$ and the $b_{\mathbf{G}}$ are the APW coefficients of the electron and the positron wave function, respectively, belonging to the reciprocal-lattice vector $\mathbf{G}$, and r_{MT} is the muffin-tin radius. The functions R_ℓ and $R_{+,\ell}$ are the solutions of the radial Schrödinger equation in the electron and positron muffin-tin potential, respectively, $j_\ell(x)$ means a spherical Bessel function, and $Y_{\ell m}(\mathbf{x})$ denotes a spherical harmonics. $E_n(E_+)$ means the energy eigenvalue of the electron(positron) state.

The quality of the APW wave functions, especially their quantum mechanically correct behavior on the surface of the muffin-tin sphere, is mainly determined by two parameters, (1) by the number $N_{\mathbf{G}}$ of reciprocal-lattice vectors $\mathbf{G}$ and (2) by $\ell_{\max}$, the number of partial waves included in the calculation. For the present work, $N_{\mathbf{G}} = 87$ (89) for bcc (fcc) metals and $\ell_{\max} = 11$ were used both for the electron and the "true" positron wave functions. This choice of $N_{\mathbf{G}}$ and $\ell_{\max}$ turned out to be sufficient for the following investigations. We shall come back to this point in detail at the beginning of Sec. IV.

III. APPROXIMATIONS OF THE APW POSITRON WAVE FUNCTION

A. Approximations of Loucks and Hubbard-Mijnarends

Apart from some reservations due to the relatively crude treatment of the crystal potentials as muffin-tin potentials, the formulas (3)–(6) can be considered as well-proved representations of the Bloch wave functions of electrons and positrons in crystalline solids. Therefore, in calculating the MDAP, it would be highly desirable to use these APW functions without any further approximation. However, an uncompromising use of Eqs. (3)–(6) in Eq. (2), as it has been performed by Gupta and Siegel,[12,13] leads to an expression which is too complicated for many practical purposes. For this reason, many authors whose positron work is based on the APW formalism (or other related formalisms) use simplifications of the positron wave function, mainly by a partial or total

neglect of the anisotropy of ψ_+ (see, for example, Refs. 8, 11, 14, 18, and 28).

One of these approximations of ψ_+ goes back to Loucks,[8] who assumed this function to be constant in the interstitial region and to be the ground-state solution of the radial Schrödinger equation including appropriate boundary conditions inside the muffin-tin sphere. A modified procedure follows from the work of Hubbard and Mijnarends:[16–18] For $|\mathbf{r}| \leq r_{\mathrm{MT}}$, a plane-wave expansion of ψ_+ is replaced by its spherical average, while in the interstitial region, the full PW expansion is used. Both proposals can easily be applied to an APW expansion of ψ_+ (see, e.g., Ref. 14). For $|\mathbf{r}| \leq r_{\mathrm{MT}}$, $\psi_+(\mathbf{r})$ is replaced by its spherical average $\psi_{\mathrm{sph}}(r)$. Mathematically, that means that $\ell_{\max}$ in the positron formula Eq. (6) is taken to be zero, and only the s part of the expansion is left. One gets

$$\psi_{\mathrm{sph}}(r) = \frac{1}{\sqrt{V}} \sum_{\mathbf{G}} b_{\mathbf{G}}\, j_0(|\mathbf{G}| r_{\mathrm{MT}}) \frac{R_{+,0}(r, E_+)}{R_{+,0}(r_{\mathrm{MT}}, E_+)} \,. \tag{7}$$

Outside the muffin-tin sphere, according the proposal of Loucks,[8] ψ_+ is approximated by the first (constant) term of Eq. (5), and the positron wave function reads

$$\psi_+^{(0)}(\mathbf{r}) = \begin{cases} \dfrac{1}{\sqrt{V}} b_0 & \text{for } |\mathbf{r}| > r_{\mathrm{MT}} \,, \\ \psi_{\mathrm{sph}}(r) & \text{for } |\mathbf{r}| \leq r_{\mathrm{MT}} \,. \end{cases} \tag{8}$$

If the full APW expansion [Eq. (5)] is used in the interstitial region, one gets the approximation[18]

$$\psi_+^{(1)}(\mathbf{r}) = \begin{cases} \dfrac{1}{\sqrt{V}} \displaystyle\sum_{\mathbf{G}} b_{\mathbf{G}} \exp(i\mathbf{G}\cdot\mathbf{r}) & \text{for } |\mathbf{r}| > r_{\mathrm{MT}} \,, \\ \psi_{\mathrm{sph}}(r) & \text{for } |\mathbf{r}| \leq r_{\mathrm{MT}} \,. \end{cases} \tag{9}$$

Here and henceforth, the superscripts (0) and (1) mean approximations of the positron wave function according to Loucks and Hubbard-Mijnarends, respectively. The corresponding expressions of $A_n(\mathbf{k}, \mathbf{p})$ can be obtained by inserting Eqs. (3), (4), (8), and (9) into Eq. (2). One gets

$$A_n^{(0)}(\mathbf{k}, \mathbf{p}) = \delta(\mathbf{p} - \mathbf{k} - \mathbf{K}) \sum_{\mathbf{G}} a_{\mathbf{G}}(\mathbf{k}) \Bigg[b_0 \left(\delta(\mathbf{G} - \mathbf{K}) - \frac{4\pi r_{\mathrm{MT}}^2}{\Omega} \frac{j_1(|\mathbf{G} - \mathbf{K}| r_{\mathrm{MT}})}{|\mathbf{G} - \mathbf{K}|} \right) + \frac{4\pi\sqrt{V}}{\Omega} \sum_{\ell=0}^{\ell_{\max}} (2\ell + 1) j_\ell(|\mathbf{k} + \mathbf{G}|) P_\ell(\cos\theta_{\mathbf{G}})\, T_\ell(p, E_n) \Bigg] \tag{10}$$

and

$$A_n^{(1)}(\mathbf{k}, \mathbf{p}) = \delta(\mathbf{p} - \mathbf{k} - \mathbf{K}) \sum_{\mathbf{G}} a_{\mathbf{G}}(\mathbf{k}) \Bigg[\sum_{\mathbf{G}'} b_{\mathbf{G}'} \left(\delta(\mathbf{G} + \mathbf{G}' - \mathbf{K}) - \frac{4\pi r_{\mathrm{MT}}^2}{\Omega} \frac{j_1(|\mathbf{G} + \mathbf{G}' - \mathbf{K}| r_{\mathrm{MT}})}{|\mathbf{G} + \mathbf{G}' - \mathbf{K}|} \right) + \frac{4\pi\sqrt{V}}{\Omega} \sum_{\ell=0}^{\ell_{\max}} (2\ell + 1) j_\ell(|\mathbf{k} + \mathbf{G}|) P_\ell(\cos\theta_{\mathbf{G}})\, T_\ell(p, E_n) \Bigg] \,, \tag{11}$$

where $\theta_{\mathbf{G}}$ is the angle between the vectors $\mathbf{k} + \mathbf{G}$ and $\mathbf{p}$, and

$$T_\ell(p, E_n) = \int_{r=0}^{r_{\mathrm{MT}}} dr\, r^2 j_\ell(pr) \frac{R_\ell(r, E_n)}{R_\ell(r_{\mathrm{MT}}, E_n)} \psi_{\mathrm{sph}}(r) \,.$$

Inserting $A_n^{(0)}$ or $A_n^{(1)}$ into Eq. (1), one gets $\rho_{\mathrm{IPM}}^{(0)}$ or $\rho_{\mathrm{IPM}}^{(1)}$, respectively, two of the most frequently used approximations of the MDAP within the IPM.

The quality of $\psi_+^{(0)}$ and $\psi_+^{(1)}$ is shown in the Figs. 1 and 2 where the true positron wave functions [Eqs. (5) and (6)] for rubidium (as an example of an alkali metal) and palladium (as an example of a transition metal with d bands) are compared with the corresponding approximations of Loucks [(Eq. 8)] and Hubbard-Mijnarends [(Eq. 9)] along the principal crystallographic directions [100], [110], and [111].

For small values of $|\mathbf{r}|$, both $\psi_+^{(0)}$ and $\psi_+^{(1)}$ are very reliable. This is by no means a surprise because of the fact that, in the vicinity of a nucleus, the positron ground state is nearly spherically symmetrical and therefore very similar to the spherically averaged function $\psi_{\mathrm{sph}}(r)$. For higher values of $|\mathbf{r}|$, however, the anisotropy of the positron wave function and, consequently, the deviations of $\psi_+^{(0)}$ and $\psi_+^{(1)}$ from ψ_+ become more and more significant. Outside the muffin-tin sphere, the approximation $\psi_+^{(0)}$ also deviates considerably from ψ_+, whereas $\psi_+^{(1)}$ exactly coincides with the true positron wave function.

It is the aim of this paper to investigate for some metals (alkali metals, transition metals, noble metals), if and to what extent these deviations influence the calculated MDAP results. For this purpose, it is necessary to develop a more accurate approximation of the positron wave function (if one does not want to use the relatively complicated MDAP formula as it can be found in Ref. 13).

B. Improved approximation

We propose the following procedure.

(i) Firstly, starting from the true positron APW expansion, a set of plane-wave coefficients $c_{\mathbf{G}}$

$$\frac{1}{\sqrt{V}}\sum_{\mathbf{G}'} b_{\mathbf{G}'}|\mathbf{G}'_{\mathrm{APW}}\rangle = \frac{1}{\sqrt{V}}\sum_{\mathbf{G}} c_{\mathbf{G}}\exp(i\mathbf{G}\cdot\mathbf{r}) \tag{12}$$

is calculated [the abbreviation $|\mathbf{G}'_{APW}\rangle$ means the $\mathbf{G}'$th term of the sums in Eqs. (5) and (6)]. To our experience, the PW expansion (12) requires only a relatively small number of terms to produce a very good description of the positron wave function not only in the interstitial region outside the muffin-tin sphere (this is self-evident due to the basic structure of the APW ansatz), but also in a certain region of r below r_{MT} where the approximations $\psi_+^{(0)}$ and $\psi_+^{(1)}$ fail. To be specific, for this work, we used 135 plane waves for bcc and 137 plane waves for fcc metals.

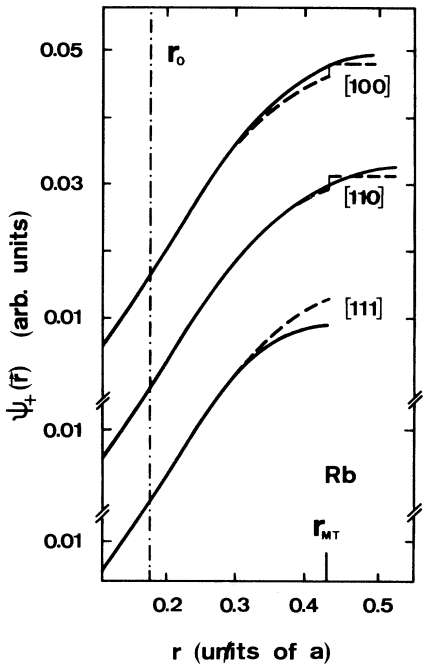

FIG. 1. APW positron wave functions of Rb along the directions [100], [110], and [111] as a function of r (in units of the lattice constant a). The units of the ordinate are arbitrary. The solid lines mean the "true" positron wave function according to Eqs. (5) and (6), and the dashed lines represent the simple approximation of the wave function Eq. (8), proposed by Loucks (Ref. 8). The approximation Eq. (9), proposed by Hubbard-Mijnarends (Ref. 18) is represented by the dashed curves up to the muffin-tin radius and by the solid lines in the interstitial region. Within the accuracy of the figure, our improved approximation according to Eq. (13) cannot be distinguished from the "true" positron wave function. The coupling radius r_0 and the muffin-tin radius r_{MT} are also indicated in the figure.

(ii) Secondly, we define the following approximation of the positron APW wave function:

$$\psi_+^{(2)}(\mathbf{r};r_0) = \begin{cases} \dfrac{1}{\sqrt{V}}\displaystyle\sum_{\mathbf{G}} c_{\mathbf{G}}\exp(i\mathbf{G}\cdot\mathbf{r}) & \text{for } |\mathbf{r}| > r_0 \ , \\ \psi_{\mathrm{sph}}(r) & \text{for } |\mathbf{r}| \le r_0 \ , \end{cases} \tag{13}$$

where $\psi_{\mathrm{sph}}(r)$ is given by Eq. (7). The "coupling radius" r_0 is smaller than r_{MT}, which means that the PW part of $\psi_+^{(2)}$ extends somewhat into the muffin-tin sphere. The best values for r_0 have been determined by minimizing the expression

$$\chi^2_{(2)}(r_0) = \int d\mathbf{r}[\psi_+^{(2)}(\mathbf{r};r_0) - \psi_+(\mathbf{r})]^2 \ , \tag{14}$$

where the region of integration is the Wigner-Seitz cell, and the subscript (2) of χ^2 refers to our new approximation $\psi_+^{(2)}$. The results of this optimization of r_0 for the metals investigated are summarized in Table I. As can be seen, all r_0 values lie roughly in the region between $0.4r_{\mathrm{MT}}$ and $0.6r_{\mathrm{MT}}$.

In order to get quantitative information about the quality of $\psi_+^{(2)}$ in comparison with $\psi_+^{(0)}$ and $\psi_+^{(1)}$, we also calculated the χ^2 values for these two approximations (of course, without any optimization process):

$$\chi^2_{(i)} = \int d\mathbf{r}[\psi_+^{(i)}(\mathbf{r}) - \psi_+(\mathbf{r})]^2 \ \ (i = 0, 1) \ . \tag{15}$$

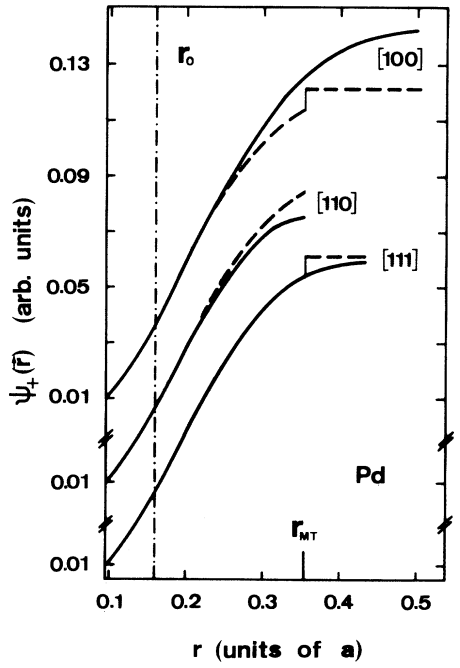

FIG. 2. APW positron wave functions of Pd along the directions [100], [110], and [111] as a function of r (in units of the lattice constant a). The units of the ordinate are arbitrary. The meaning of the curves is equal to that in Fig.1.

TABLE I. Coupling radii r_0 (in units of the muffin-tin radius r_{MT}) for the improved approximation (13) of the positron wave functions in alkali metals and in copper and palladium. The lattice constants a and the muffin-tin radii r_{MT} are given in atomic units. The meaning of $\chi^2_{(0)}$, $\chi^2_{(1)}$, and $\chi^2_{(2)}(r_0)$ is explained by Eqs. (14) and (15) and the text following these equations.

metal	a	r_{MT}	r_0/r_{MT}	$10^4\chi^2_{(2)}(r_0)$	$\chi^2_{(0)}/\chi^2_{(2)}$	$\chi^2_{(1)}/\chi^2_{(2)}$
Li	6.597	2.857	0.635	0.027 647	46.7	18.5
Na	8.003	3.465	0.635	0.040 738	51.8	20.6
K	9.882	4.279	0.494	0.008 157 5	451.8	179.8
Rb	10.554	4.570	0.410	0.005 797 0	788.7	314.1
Cs	11.423	4.946	0.451	0.020 768	283.1	112.9
Cu	6.831	2.415	0.410	0.003 981 4	2926.6	532.9
Pd	7.42	2.62	0.451	0.031 344	642.4	116.8

The ratio $\chi^2_{(0)}/\chi^2_{(2)}$ and $\chi^2_{(1)}/\chi^2_{(2)}$, which are also included in Table I, clearly indicate the superiority of $\psi^{(2)}_+$ over $\psi^{(0)}_+$ and $\psi^{(1)}_+$. The high quality of our approximation (13) is also demonstrated in Figs. 1 and 2. Both for rubidium and for palladium, within the accuracy of the figures, no deviation between the true function ψ_+ and our approximation $\psi^{(2)}_+$ is visible (this is also true for the other alkali metals and for copper). Therefore we think that it is well justified to consider our proposal $\psi^{(2)}_+$ as a very good approximation of the true APW positron wave function.

Inserting $\psi^{(2)}_+$ together with the APW electron wave function [Eqs. (3) and (4)] into the expression for $A_n(\mathbf{k},\mathbf{p})$, Eq. (2), one gets

$$A^{(2)}_n(\mathbf{k},\mathbf{p}) = \delta(\mathbf{p}-\mathbf{k}-\mathbf{K}) \sum_{\mathbf{G}} a_{\mathbf{G}}(\mathbf{k}) \Bigg[\sum_{\mathbf{G}'} c_{\mathbf{G}'} \left(\delta(\mathbf{G}+\mathbf{G}'-\mathbf{K}) - \frac{4\pi r^2_{MT}}{\Omega} \frac{j_1(|\mathbf{G}+\mathbf{G}'-\mathbf{K}|r_{MT})}{|\mathbf{G}+\mathbf{G}'-\mathbf{K}|} \right) + \frac{4\pi\sqrt{V}}{\Omega} \sum_{\ell} (2\ell+1) j_\ell(|\mathbf{k}+\mathbf{G}|r_{MT}) P_\ell(\cos\theta_{\mathbf{G}})\, U_\ell(p,E_n) + \frac{4\pi}{\Omega} \sum_{\mathbf{G}'} c_{\mathbf{G}'} \sum_{\ell} (2\ell+1) j_\ell(|\mathbf{k}+\mathbf{G}|r_{MT}) P_\ell(\cos\theta_{\mathbf{G},\mathbf{G}'})\, W_\ell(|\mathbf{p}-\mathbf{G}'|,E_n) \Bigg], \tag{16}$$

where

$$U_\ell(p,E_n) = \int_{r=0}^{r_0} dr\, r^2 j_\ell(pr) \frac{R_\ell(r;E_n)}{R_\ell(r_{MT};E_n)} \psi_{sph}(r)$$

and

$$W_\ell(|\mathbf{p}-\mathbf{G}'|,E_n) = \int_{r=r_0}^{r_{MT}} dr\, r^2 j_\ell(|\mathbf{p}-\mathbf{G}'|r) \times \frac{R_\ell(r;E_n)}{R_\ell(r_{MT};E_n)} .$$

$\theta_{\mathbf{G}}$ has been already defined in context with Eq. (11), and $\theta_{\mathbf{G},\mathbf{G}'}$ means the angle between the vectors $\mathbf{k}+\mathbf{G}$ and $\mathbf{p}-\mathbf{G}'$. The expression (16) has the same structure as Eq. (11), except for an additional term due to the new definition of the positron wave function between the coupling radius r_0 and the muffin-tin radius according to Eq. (13). Of course, this term causes a considerable increase of the computation time [roughly a factor of 2–3 in comparison with a numerical evaluation of Eq. (11)], but we think that this is acceptable if one takes into account the significantly improved approximation of the positron wave function used in Eq. (16). Consequently, the insertion of $A^{(2)}_n$ into Eq. (1) leads to the very reliable approximation $\rho^{(2)}_{IPM}$ of the true MDAP.

The main role of Eq. (16) for the present investigation is that it may be used for a critical examination of the MDAP approximations $\rho^{(0)}_{IPM}$ and $\rho^{(1)}_{IPM}$ which neglect or only partly include the anisotropy of the positron wave function. Namely, if one accepts $\rho^{(2)}_{IPM}$ as a standard, all differences

$$\Delta\rho^{(i,2)}_{IPM} \equiv \rho^{(i)}_{IPM} - \rho^{(2)}_{IPM} \quad (i=0,1) \tag{17}$$

may be considered as errors of the approximations proposed by Loucks ($i=0$) or Hubbard-Mijnarends ($i=1$). Therefore we calculated and compared $\rho^{(0)}_{IPM}$, $\rho^{(1)}_{IPM}$, and $\rho^{(2)}_{IPM}$ for some momenta inside the central BZ and inside some umklapp zones. The results of this test are summarized in the Tables II and III and in Figs. 3 and 4. They are discussed in the following section.

TABLE II. A comparison of the approximations $\rho^{(i)}_{\mathrm{IPM}}$ [$i = 0$, Loucks (Ref. 8); $i = 1$, Hubbard-Mijnarends (Ref. 18); $i = 2$, this work] of the momentum density of annihilation pairs (MDAP), based on Eqs. (10), (11), and (16), respectively, for the alkali metals Li, Na, K, Rb, and Cs. The MDAP has been calculated for the Γ point of the Brillouin zones belonging to the reciprocal-lattice vectors $\mathbf{G} = (0,0,0)$, (1,1,0), and (2,0,0) ($\mathbf{G}$ in units of $2\pi/a$, a being the lattice constant). $\Delta\rho^{(i,2)}_{\mathrm{IPM}}$ means the differences between $\rho^{(i)}_{\mathrm{IPM}}$ and $\rho^{(2)}_{\mathrm{IPM}}$; the values in parentheses are the corresponding relative errors (in %) with respect to $\rho^{(2)}_{\mathrm{IPM}}$.

metal	G	$\rho^{(2)}_{\mathrm{IPM}}$	$\Delta\rho^{(0,2)}_{\mathrm{IPM}}$	$\Delta\rho^{(1,2)}_{\mathrm{IPM}}$
Li	(0,0,0)	0.949 800	+0.000 069 (+0.007)	+0.000 027 (+0.003)
	(1,1,0)	0.006 091 29	−0.000 088 62 (−1.45)	−0.000 036 50 (−0.60)
	(2,0,0)	0.000 695 85	+0.000 196 86 (+28.3)	+0.000 099 12 (+14.2)
Na	(0,0,0)	0.963 386	+0.000 249 (+0.026)	+0.000 091 (+0.009)
	(1,1,0)	0.005 465 46	−0.000 101 29 (−1.85)	−0.000 041 94 (−0.77)
	(2,0,0)	0.000 643 76	+0.000 243 83 (+37.9)	+0.000 123 13 (+19.1)
K	(0,0,0)	0.947 217	+0.000 334 (+0.035)	+0.000 122 (+0.013)
	(1,1,0)	0.009 314 73	−0.000 179 33 (−1.93)	−0.000 074 81 (−0.80)
	(2,0,0)	0.000 647 74	+0.000 340 07 (+52.5)	+0.000 169 45 (+26.2)
Rb	(0,0,0)	0.940 561	+0.000 406 (+0.043)	+0.000 157 (+0.017)
	(1,1,0)	0.010 886 6	−0.000 228 4 (−2.10)	−0.000 101 9 (−0.94)
	(2,0,0)	0.000 596 59	+0.000 371 17 (+62.2)	+0.000 182 82 (+30.6)
Cs	(0,0,0)	0.924 990	+0.000 307 (+0.033)	+0.000 093 (+0.010)
	(1,1,0)	0.014 272 7	−0.000 310 0 (−2.17)	−0.000 139 8 (−0.98)
	(2,0,0)	0.000 412 10	+0.000 370 06 (+89.8)	+0.000 176 49 (+42.8)

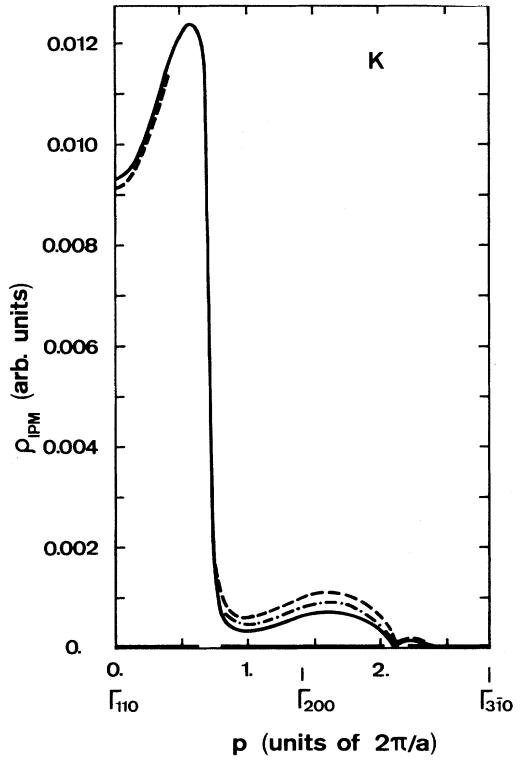

FIG. 3. The momentum densities of annihilation pairs ρ_{IPM} in K for the (110) and (200) umklapp regions, calculated within the independent-particle model. The horizontal coordinate axis has the $[1\bar{1}0]$ direction with Γ_{110} as zero. The marked parts of this axis indicate the regions of occupied electron states. The solid line represents the improved approximation $\rho^{(2)}_{\mathrm{IPM}}$ (this work), the dashed and the dash-dotted lines show the approximations $\rho^{(0)}_{\mathrm{IPM}}$ and $\rho^{(1)}_{\mathrm{IPM}}$ according to Loucks (Ref. 8) and Hubbard-Mijnarends (Ref. 18), respectively.

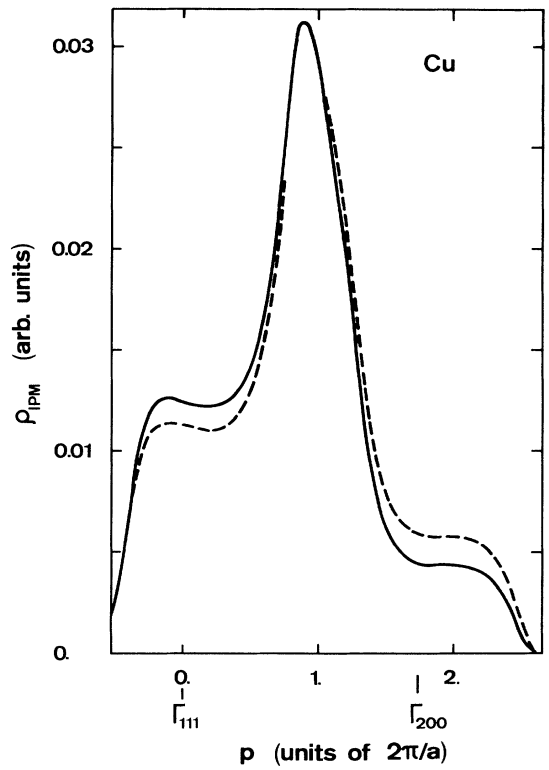

FIG. 4. The momentum densities of annihilation pairs ρ_{IPM} in Cu (electron states with predominant $s + p$ character) for the (111) and (200) umklapp regions, calculated within the independent-particle model. The horizontal coordinate axis has the $[1\bar{1}\bar{1}]$ direction with Γ_{111} as zero. The solid line represents the improved approximation $\rho^{(2)}_{\mathrm{IPM}}$ (this work), the dashed line shows the approximation $\rho^{(0)}_{\mathrm{IPM}}$ according to Loucks (Ref. 8).

TABLE III. A comparison of the approximations $\rho_{\mathrm{IPM}}^{(i)}$ [$i = 0$, Loucks (Ref. 8); $i = 1$, Hubbard-Mijnarends (Ref. 18); $i = 2$, this work] of the momentum density of annihilation pairs (MDAP), based on Eqs. (10), (11), and (16), respectively, for Cu and Pd. The MDAP has been calculated for the momenta defined by Eq. (18). For both metals, the calculation has been performed for two distinct electron states, one of them with a predominant $s + p$ and the other one with a predominant d character (notice the charge analysis of the corresponding states). $\Delta\rho_{\mathrm{IPM}}^{(i,2)}$ means the differences between $\rho_{\mathrm{IPM}}^{(i)}$ and $\rho_{\mathrm{IPM}}^{(2)}$; the values in parentheses are the corresponding relative errors (in %) with respect to $\rho_{\mathrm{IPM}}^{(2)}$.

G	$\rho_{\mathrm{IPM}}^{(2)}$	$\Delta\rho_{\mathrm{IPM}}^{(0,2)}$	$\Delta\rho_{\mathrm{IPM}}^{(1,2)}$
	Cu (predominant $s + p$ character): $s = 87.9\%, p = 11.0\%, d = 1.1\%$		
(0,0,0)	0.934 482	+0.001 269 (+0.136)	+0.000 284 (+0.030)
(1,1,1)	0.008 443 11	−0.001 005 62 (−11.9)	−0.000 261 45 (−3.1)
(2,0,0)	0.004 860 18	+0.001 477 29 (+30.4)	+0.000 351 84 (+7.2)
	Cu (predominant d character): $s = 0.2\%, p = 1.8\%, d = 96.8\%$		
(0,0,0)	0.005 039 76	−0.000 075 10 (−1.49)	−0.000 022 76 (−0.45)
(1,1,1)	0.127 436	+0.001 860 (+1.46)	+0.000 836 (+0.66)
(2,0,0)	0.002 046 33	−0.000 082 23 (−4.02)	−0.000 018 72 (−0.91)
	Pd (predominant $s + p$ character): $s = 84.3\%, p = 9.5\%, d = 6.2\%$		
(0,0,0)	0.867 385	+0.001 526 (+0.176)	+0.000 341 (+0.039)
(1,1,1)	0.001 809 75	−0.000 664 72 (−36.7)	−0.000 192 94 (−10.7)
(2,0,0)	0.006 843 71	+0.002 396 38 (+35.0)	+0.000 547 04 (+8.0)
	Pd (predominant d character): $s = 3.1\%, p = 4.4\%, d = 90.2\%$		
(0,0,0)	0.043 048 4	−0.000 380 7 (−0.88)	−0.000 119 8 (−0.28)
(1,1,1)	0.226 721	+0.003 661 (+1.61)	+0.001 845 (+0.81)
(2,0,0)	0.002 893 08	−0.000 340 22 (−11.8)	−0.000 077 15 (−2.7)

IV. RESULTS AND DISCUSSION

Before we discuss in detail the errors $\Delta\rho_{\mathrm{IPM}}^{(i,2)}$ which arise if one of the approximations $\psi_+^{(0)}$ or $\psi_+^{(1)}$ is used in the MDAP formulas (1) and (2), we have to make sure that the calculated ρ_{IPM}'s are not falsified by a nonsufficient convergence of the APW wave functions. Therefore we made extensive convergence tests, and we observed that an increase of $N_{\mathbf{G}}$ and $\ell_{\max}$ used in this work (see the end of Sec. II) may indeed slightly change some of the numbers of the Tables II and III. However, it must be emphasized that these uncertainties of the $\Delta\rho_{\mathrm{IPM}}$ values are at least one order (and in most cases two orders) of magnitude smaller than the corresponding $\Delta\rho_{\mathrm{IPM}}$ values themselves, which means that $N_{\mathbf{G}} = 87(89)$ and $\ell_{\max} = 11$ used in our calculations guarantee that all absolute and relative errors presented in Tables II and III are significant.

In Table II, we compare the approximations $\rho_{\mathrm{IPM}}^{(0)}$ and $\rho_{\mathrm{IPM}}^{(1)}$ with our standard $\rho_{\mathrm{IPM}}^{(2)}$ for the MDAP due to valence electrons in alkali metals at the Γ point of the central BZ, $\mathbf{G} = (0,0,0)$, and of the nearest umklapp zones belonging to the reciprocal-lattice vectors $\mathbf{G} = (1,1,0)$ and (2,0,0).

It is one striking feature of the results of Table II that the values of $\Delta\rho_{\mathrm{IPM}}^{(0,2)}$ and $\Delta\rho_{\mathrm{IPM}}^{(1,2)}$ (the absolute errors of $\rho_{\mathrm{IPM}}^{(0)}$ and $\rho_{\mathrm{IPM}}^{(1)}$, respectively) do not show a very strong dependence on the different metals or on the different regions in the momentum space. In fact, between the lowest and the highest values of $\Delta\rho_{\mathrm{IPM}}^{(i,2)}$ ($i = 0,1$), a ratio of about 1:6 is observed, in strong contrast to the corresponding ratio of the ρ_{IPM} values themselves which amounts to more than 1:2000. For instance, in the case of rubidium, the absolute values of $\Delta\rho_{\mathrm{IPM}}^{(0,2)}$ for the (000), (100), and (200) regions approximately amount to 4.1×10^{-4}, 2.3×10^{-4}, and 3.7×10^{-4}, respectively, while the corresponding values of $\rho_{\mathrm{IPM}}^{(2)}$ are 0.94, 0.0109, and 0.000 597.

The consequence of this behavior of the absolute errors is, of course, a strong increase of the corresponding relative errors with decreasing ρ_{IPM}. Therefore, for all alkali metals investigated, the reliability of the approximation $\rho_{\mathrm{IPM}}^{(0)}$ is very high inside the central BZ (with relative errors less than 0.05%), and it is satisfying inside the nearest (110) umklapp region where the relative errors slightly increase from about 1.5% (lithium) to about 2.2% (caesium). However, the situation completely changes if we look at the results for the (200) umklapp region. In this case, the small amounts of the ρ_{IPM} values lead to high and partly dramatic relative errors of the approximation $\rho_{\mathrm{IPM}}^{(0)}$ (about 28% for Li, 38% for Na, 53% for K, 62% for Rb, and 90% for Cs). Concerning the approximation $\rho_{\mathrm{IPM}}^{(1)}$ proposed by Hubbard-Mijnarends, its qualitative error behavior is quite similar to the results discussed above. Quantitatively, however, the better performance of $\psi_+^{(1)}$ in the interstitial region leads to absolute and relative errors of $\rho_{\mathrm{IPM}}^{(1)}$ which are only about half the corresponding errors of the approximation $\rho_{\mathrm{IPM}}^{(0)}$.

As an instructive example which is typical for all alkali metals investigated in this paper, the ρ_{IPM} values in

potassium along the [1$\bar{1}$0] direction in momentum space are shown in Fig. 3. Because of the fact that—as has been discussed before—the central momentum region is almost insensitive to an anisotropy effect of ψ_+, only the (110) umklapp region with its rather small and the (200) umklapp region with its remarkably high sensitivity on the anisotropy of the positron wave function are shown in this figure.

Until now, we discussed the annihilation behavior of strongly delocalized valence electrons in alkali metals. Such electrons have a considerable probability density in the interstitial space as well as in the region at and under the surface of the muffin-tin sphere, essentially within the sensitive region of $|\mathbf{r}| > r_0$ where the approximations $\psi_+^{(0)}$ and $\psi_+^{(1)}$ show relatively large deviations from the true positron wave function (see Figs. 1 and 2). In d-band metals like copper and palladium, however, there are also stronger localized electron states (with predominant d character) near to the Fermi level. These d electrons have their highest probability density in the interior parts of the muffin-tin sphere (where the anisotropy of ψ_+ is very small), and we should therefore expect a significant reduction of $\Delta\rho_{\mathrm{IPM}}^{(0)}$ and $\Delta\rho_{\mathrm{IPM}}^{(1)}$.

This is exactly what one observes from Table III where MDAP values for copper and palladium for the momenta

$$\mathbf{p} = -\frac{0.3}{\sqrt{3}}(1,1,1) + \mathbf{G} \tag{18}$$

(in units of $2\pi/a$, a being the lattice constant) with $\mathbf{G} = (0,0,0)$, (1,1,1), and (2,0,0) are summarized. For these metals, the calculations were performed for two distinct electron states, one with a predominant $s+p$ character and one with a predominant d character (notice the charge analysis of these electron states in Table III). As can be seen from this table, for electrons of marked $s+p$ character, the error behavior of $\rho_{\mathrm{IPM}}^{(0)}$ and $\rho_{\mathrm{IPM}}^{(1)}$ is similar to that for the alkali metals. One observes very low relative errors for the central momentum region, and considerable relative errors for the (111) and (200) umklapp regions, especially for $\rho_{\mathrm{IPM}}^{(0)}$. The better performance of $\rho_{\mathrm{IPM}}^{(1)}$ with respect to $\rho_{\mathrm{IPM}}^{(0)}$ is more marked than it was in the case for the alkali metals, with a ratio of the corresponding errors of about 1:4. In Fig. 4, we show the $\rho_{\mathrm{IPM}}^{(2)}$ and the $\rho_{\mathrm{IPM}}^{(0)}$ values in copper along a line in momentum space through the Γ points of the (111) and (200) umklapp regions. The $\rho_{\mathrm{IPM}}^{(1)}$ values are not included in Fig. 4, because the corresponding curve is very similar to the $\rho_{\mathrm{IPM}}^{(2)}$ curve and would diminish the clearness of the figure.

For electrons with predominant d character, both the absolute and the relative errors of $\rho_{\mathrm{IPM}}^{(0)}$ and $\rho_{\mathrm{IPM}}^{(1)}$ are significantly smaller for the whole momentum region investigated. This reduction is presumably even stronger for tightly localized core electrons, but we did not perform any tests in this direction.

V. CONCLUSIONS

As a consequence of our numerical tests concerning the quality of the frequently used approximations $\rho_{\mathrm{IPM}}^{(0)}$ and $\rho_{\mathrm{IPM}}^{(1)}$ for the MDAP, we can conclude the following. These approximations are excellent for momenta within the central BZ and fairly good for momenta near to the central zone [e.g., for the (110) zones in bcc metals]. For higher momenta, however [e.g., for the (200) zones in bcc and the (111) and (200) zones in fcc metals], the situation considerably deteriorates, especially for annihilation processes of strongly delocalized electron states. In these cases, the anisotropy of the positron wave function plays an important role in an accurate calculation of the MDAP. Therefore, for theoretical investigations of the MDAP and for comparisons between theoretical and experimental annihilation rates where the momenta do not go very far beyond the central region, the accuracy of the approximations of ψ_+ according to Loucks [Eq.

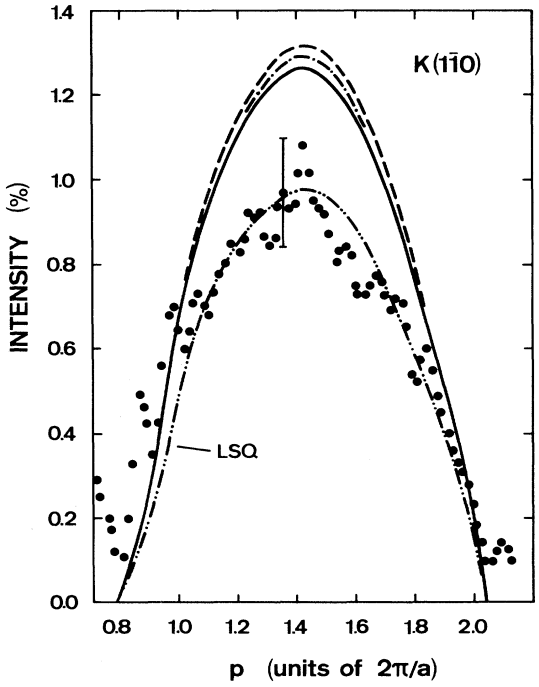

FIG. 5. The influence of the anisotropy of ψ_+ on a 2D-ACPAR projection profile of the momentum density of annihilation pairs onto the (1$\bar{1}$0) plane in K. The horizontal axis has the [110] direction with Γ_{000} as zero. The circles represent the experimental results of Oberli (Ref. 29). The solid line shows the IPM profile according to the improved approximation $\rho_{\mathrm{IPM}}^{(2)}$ (this work). The dashed and the dash-dotted lines belong to the approximations $\rho_{\mathrm{IPM}}^{(0)}$ and $\rho_{\mathrm{IPM}}^{(1)}$, according to the formulas of Loucks (Ref. 8) and Hubbard-Mijnarends (Ref. 18), respectively. The line indicated by LSQ is the result of a least-squares scaling of the IPM profile onto the experimental points. All results are given as a fraction of the conduction-electron contribution at $p_x = p_y = 0$.

(8)] and Hubbard-Mijnarends [Eq. (9)] will generally be sufficient. As an example which supports this argumentation, in Fig. 5, we show a comparison of theoretical and experimental results based on measurements of the two-dimensional angular correlation of positron annihilation radiation (2D-ACPAR) in potassium. For that, numerical integrations of the calculated ρ_{IPM} values along high-symmetry directions in the momentum space were performed (of course, only regions of occupied electron states were taken into account for these integrations), and these results were compared with corresponding experimental data of Oberli.[29] As can be seen in Fig. 5, the anisotropy effect of ψ_+, indicated by the three theoretical curves based on $\rho^{(i)}_{\mathrm{IPM}}$ $(i = 0, 1, 2)$, is indeed not negligible, but it is smaller than the statistical uncertainties of the experimental values and considerably smaller than the difference between the experimental and theoretical profiles which is mainly due to many-body effects.

In order to understand the smallness of this anisotropy effect, one has to remember that the theoretical 2D-ACPAR curves of Fig. 5 result from integrations of ρ_{IPM} curves like those in Fig. 3. Obviously, by far the greatest part to these integrals (about 90%) comes from ρ_{IPM} values of the (110) umklapp region, and only a small rest of about 10% is due to the (200) umklapp region. Therefore, despite the high sensibility of this region on different approximations of ψ_+, the total anisotropy effect on the (integrated) $(1\bar{1}0)$ ACPAR profile is relatively small.

However, this is certainly no more true if one considers 2D-ACPAR profiles where the (200) umklapp regions become dominant (regrettably, for such high-momentum regions, there is a lack of experimental data with sufficient statistical quality due to the small intensities of the corresponding annihilation rates). In these cases, the anisotropy effect of ψ_+ might be even more important than many-body effects, but our present knowledge about the influence of electron-positron correlations on high-momentum components of the annihilation rate is not yet good enough to make a final decision about this question.

Therefore, if one is interested in investigations of the MDAP in the high-momentum region, as, for example, we were in our recent paper,[25] it is of great importance to use an efficient and reliable approximation of the positron wave function like the expression (13) that we propose in this paper.

ACKNOWLEDGMENTS

The author is grateful to Dr. M. Šob for many helpful discussions and for his continuing interest in this work.

[1] S. Berko and J.S. Plaskett, Phys. Rev. **112**, 1877 (1958).
[2] D. Stroud and H. Ehrenreich, Phys. Rev. **171**, 399 (1968).
[3] A.G. Gould, R.N. West, and B.G. Hogg, Can. J. Phys. **50**, 2294 (1972).
[4] H.P. Bonde, S.B. Shrivastava, and K.P. Joshi, Solid State Commun. **41**, 683 (1982).
[5] P. Kubica and M.J. Stott, J. Phys. F **4**, 1969 (1974).
[6] M.J. Stott and P. Kubica, Phys. Rev. B **11**, 1 (1975).
[7] G. Kögel (unpublished).
[8] T.L. Loucks, Phys. Rev. **144**, 504 (1966).
[9] H. Bross and H. Stöhr, Appl. Phys. **3**, 307 (1974).
[10] S. Wakoh, Y. Kubo, and J. Yamashita, J. Phys. Soc. Jpn. **38**, 416 (1975).
[11] K. Iyakutti and V. Devanathan, J. Phys. C **10**, 825 (1977).
[12] R.P. Gupta and R.W. Siegel, Phys. Rev. Lett. **39**, 1212 (1977).
[13] R.P. Gupta and R.W. Siegel, Phys. Rev. B **22**, 4572 (1980).
[14] A. Kshirsagar and D.G. Kanhere, Phys. Rev. B **34**, 853 (1986).
[15] J. Hubbard, J. Phys. C **2**, 1222 (1969).
[16] J. Hubbard and P.E. Mijnarends, J. Phys. C **5**, 2323 (1972).
[17] P.E. Mijnarends, Physica (Amsterdam) **63**, 235 (1973); **63**, 248 (1973).
[18] P.E. Mijnarends, in *Positrons in Solids*, edited by P. Hautojärvi (Springer-Verlag, Berlin, 1979), pp. 42ff.
[19] A.K. Singh and T. Jarlborg, J. Phys. F **15**, 727 (1985).
[20] P. E. Mijnarends and L. P. L. M. Rabou, J. Phys. F **16**, 483 (1986).
[21] P. E. Mijnarends and A. Bansil, J. Phys. Condens. Matter **2**, 911 (1990).
[22] K. E. H. M. Hanssen and P. E. Mijnarends, Phys. Rev. B **34**, 5009 (1986).
[23] V. Sundararajan, D.G. Kanhere, and J. Callaway, Phys. Lett. A **133**, 521 (1988).
[24] M.J. Puska, Phys. Status Solidi A **102**, 11 (1987).
[25] H. Sormann and M. Šob, Phys. Rev. B **41**, 10529 (1990).
[26] L. Hedin and B. I. Lundqvist, J. Phys. C **4**, 2064 (1971).
[27] V. L. Moruzzi, J. F. Janak, and A. R. Williams, *Calculated Electronic Properties of Metals* (Pergamon, New York, 1978).
[28] R.M. Singru, Pramana **2**, 299 (1974).
[29] L. Oberli, Ph.D. thesis, Université de Génève, 1985 (unpublished).